Bioorganic & Medicinal Chemistry 25 (2017) 5452–5460

Contents lists available at ScienceDirect

Bioorganic & Medicinal Chemistry

journal homepage: www.elsevier.com/locate/bmc

Exploring the C^N^C theme: Synthesis and biological properties of tridentate cyclometalated gold(III) complexes

Sophie Jürgens [a,b], Valeria Scalcon [c], Natalia Estrada-Ortiz [d], Alessandra Folda [c], Federica Tonolo [c], Christian Jandl [a], Duncan L. Browne [b], Maria Pia Rigobello [c], Fritz E. Kühn [a,*], Angela Casini [b,d,e,*]

[a] Molecular Catalysis, Catalysis Research Centre and Department of Chemistry, Technische Universität München, Lichtenbergstr. 4, 85747 Garching bei München, Germany
[b] School of Chemistry, Cardiff University, Park Place, Cardiff CF10 3AT, United Kingdom
[c] Dept. of Biomedical Sciences, University of Padova, via Ugo Bassi 58/b, 35131 Padova, Italy
[d] Dept. Pharmacokinetics, Toxicology and Targeting, University of Groningen, A. Deusinglaan 1, 9713 AV Groningen, The Netherlands
[e] Institute of Advanced Study, Technische Universität München, Lichtenbergstr. 2a, 85748 Garching bei München, Germany

ARTICLE INFO

Article history:
Received 11 June 2017
Revised 25 July 2017
Accepted 2 August 2017
Available online 9 August 2017

Keywords:
Gold(III) complexes
Cyclometalation
Anticancer agents
Thioredoxin reductase
Thiols

ABSTRACT

A family of cyclometalated Au(III) complexes featuring a tridentate C^N^C scaffold has been synthesized and characterized. Microwave assisted synthesis of the ligands has also been exploited and optimized. The biological properties of the thus formed compounds have been studied in cancer cells and demonstrate generally moderate antiproliferative effects. Initial mechanistic insights have also been gained on the gold complex [Au(C^N^C)(GluS)] (**3**), and support the idea that the thioredoxin system may be a target for this family of compounds together with other relevant intracellular thiol-containing molecules.

1. Introduction

Gold-based organometallic complexes as anti-cancer agents have become increasingly popular in recent years, and several reviews have been published highlighting their structural diversity and biological activity.[1] In fact, organometallic complexes display numerous attractive features. For example, while the organic ligand allows for the introduction of stereospecificity and alteration of the physicochemical properties by choosing different functional groups, the metal–carbon (M–C) bond provides strong *trans* influence and, in the case of π-bonded aromatic arene and cyclopentadienyl ligands, can act both as electron donors and acceptors. Furthermore, variations of the organic moiety are accessible, allowing the "fine-tuning" of the physiochemical properties of the respective metal compound. Finally, by choosing specific targeting moieties, either incorporation into the ligand or tethering to the metal centre can be achieved in a modular approach.

Typical classes of organometallics include metallocenes, metallo-arenes, metallo-carbonyls, metallo-carbenes (e.g. *N*-heterocyclic carbenes, NHC), alkynyl complexes, etc.[2] featuring both mononuclear and multinuclear scaffolds. All these compound families have been extensively applied in catalysis during the last decades.[3] However, their medicinal use has been considered only much more recently.[1c,2,4]

Concerning Au(I) organometallics, in 2008 Berners-Price et al. synthesized a series of mononuclear cationic Au(I) biscarbene complexes that show remarkable cytotoxicity *in vitro* and are able to induce mitochondrial damage.[5] Since then, the effects of Au(I) NHC complexes on cell metabolism and their interference with pathways relevant to cancer cell proliferation have been studied in a broad number of cases.[1a,4b,6]

In this context, to explore the design of Au(III) compounds for biological applications, cyclometalation is a convenient method to stabilize the otherwise easily reduced Au(III) centre, and numerous cyclometalated scaffolds have been synthesized, including C^N, C^N^C, C^N^N and C^N^S.[1b,c,7] Cyclometalated Au(III) C^N compounds of general formula **[(Au(damp)X$_2$]** (Fig. 1) with anticancer properties were first investigated by Parish, Buckley et al. in 1996,[8] featuring a 2[dimethylamino)methyl]-phenyl (damp) backbone. The compounds display cytotoxic activity which is comparable to that of cisplatin, against a variety cancer cell lines. This activity is also accompanied by high selectivity and cytotoxicity *in vitro* which translates to moderate activity *in vivo*.

* Corresponding authors at: School of Chemistry, Cardiff University, Park Place, Cardiff CF10 3AT, United Kingdom (A. Casini).
E-mail addresses: fritz.kuehn@ch.tum.de (F.E. Kühn), casinia@cardiff.ac.uk (A. Casini).

http://dx.doi.org/10.1016/j.bmc.2017.08.001
0968-0896/

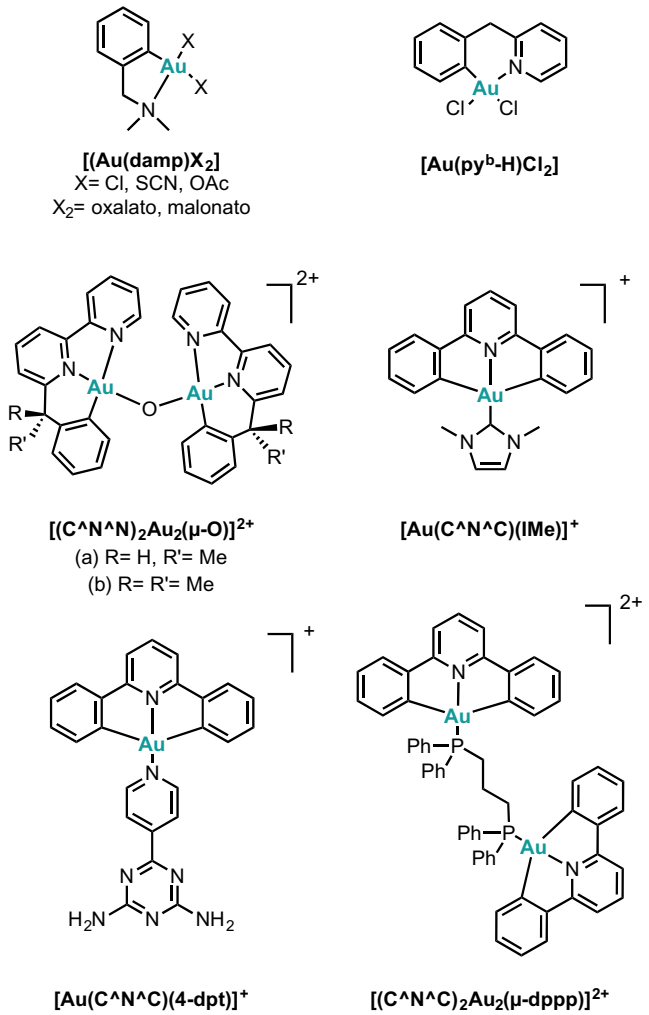

Fig. 1. Representative cyclometalated Au(III) complexes with anticancer properties.

In 1996, the synthesis of an Au(III) 2-benzylpyridine derivative **[Au(py^b-H)Cl$_2$]** (py^b-H = C^N cyclometalated 2-benzylpyridine) (Fig. 1) was reported by Cinellu et al.[9] In 2015 Casini, Cinellu et al. synthesized a structural analogue of this complex replacing the chlorido ligand, *trans* to the nitrogen atom, with 1,3,5-triaza-phosphaadamantane (PTA).[10] The resulting compound displays good cytotoxic activity against various cancer cell lines such as A2780 (human ovarian adenocarcinoma). Furthermore, dinuclear oxo-bridged Au(III) C^N^N complexes of formula **[(C^N^N)$_2$Au$_2$(μ-O)](PF$_6$)$_2$** (with C^N^N = 6-(1-methylbenzyl)-2,2'-bipyridine or 6-(1,1-dimethylbenzyl)-2,2′-bipyridine) showing moderate cytotoxicity against various cancer cell lines were synthesized.[11] (Fig. 1).

The field of Au(III) C^N^C complexes with anticancer properties has been closely examined by Che and co-workers[1 b,12] For example, dinuclear complexes of the type [Au$_m$(C^N^C)$_m$L]$^{n+}$ (with HC^N^CH = 2,6-diphenylpyridine; m = 1–3; n = 0–3) showed higher cytotoxic activity against various cancer cell lines than their mononuclear counterparts.[12]

The highest cytotoxicities were observed for complex **[Au$_2$(C^N^C)$_2$(μ-dppp)](OTf)$_2$** (Fig. 1), relating to the cytotoxicity of the free 1,2-bis(diphenylphosphino)propane (dppp) ligand. By replacing the phosphane moiety with an NHC ligand as in the cationic C^N^C stabilized complexes [Au$_n$(R–C^N^C)$_n$(NHC)]$^{n+}$, a general decrease in cytotoxic effects has been noted,[13] supporting the idea that indeed phosphine ligand-mediated cytotoxicity plays a major role in the overall anticancer properties. Nevertheless, within this series, the mononuclear complex **[Au(C^N^C)(IMe)]CF$_3$SO$_3$** (IMe = 1,3-dimethylimidazol-2-ylidene) (Fig. 1) shows higher cytotoxic activity than its dinuclear analogue, and a high degree of selectivity towards human cancer cells compared to normal lung fibroblasts (CCD-19Lu). Through DNA interaction studies it was demonstrated that the compound induces DNA strand breaks and can cause subsequent cell death through the stabilization of Topoisomerase-linked DNA.[14] Treatment of nude mice bearing PLC tumors (hepatocellular carcinoma) with **[Au(C^N^C)(IMe)]CF$_3$SO$_3$** at 10 mg/kg/week for 28 days significantly suppressed (47%) tumor growth when compared with that of the vehicle control.[13]

Of note from the same group, is the application of supramolecular polymers, self-assembled from cyclometalated Au(III) C^N^C complexes, as anticancer agents. The mononuclear complex **[Au(C^N^C)(4-dpt)]$^+$** (C^N^C = 2,6-diphenylpyridine, 4-dpt = 2,4-diamino-6-(4-pyridyl)-1,3,5-triazine) (Fig. 1) was chosen due to the ability of the antiangiogenic 4-dpt ligand to form intramolecular hydrogen bonds and to establish π-π interactions, leading to supramolecular complex formation by self-assembly at ambient temperatures.[15] The supramolecular polymer displays high cytotoxic activity towards B16 cells (murine cancer).

In terms of possible mechanisms of action, cytotoxic Au(III) complexes can interact with protein targets,[16] including those constituting the thioredoxin system, often overexpressed in tumor cells and involved in maintaining the intracellular redox balance.[17] Among the enzymes included in this system, the seleno-protein thioredoxin reductase (TrxR) contains a cysteine-selenocysteine redox pair at the C-terminal active site, and the solvent-accessible selenolate group, arising from enzymatic reduction, constitutes a likely target for "soft" metal ions such as gold. In addition, Au(III) complexes can interfere with thiols including glutathione, the most abundant intracellular reducing agent.

Within the scope of new medicinally relevant organometallic Au(III) compounds, two new cyclometalated Au(III) complexes of the general formula [Au(III)(C^N^C)X] (with C^N^C = 2,6-diphenylpyridine and X = Cl, thio-β-D-glucose-tetraacetate (GluS), 1,3,5-triazaphosphaadamantane (PTA)) were synthesized. The complexes were prepared starting from the literature known chlorido precursor [Au(III)(C^N^C)Cl][18] (Fig. 2, **1**), substituting the chlorido ligand with PTA (**2**) and thio-β-D-glucose-tetraacetate (GluSH) (**3**), respectively. The PTA ligand was chosen to increase the water solubility, while the GluS$^-$ ligand was selected as modulator of the hydrophilic/lipophilic character, as well as a possible facilitator of the compound's uptake via interactions with the GLUT1 transporter. A second series of analogous C^N^C complexes – Au(III)[(C^N^R^C)] – was synthesized starting from the corresponding 2,4,6-triarylpyridine ligands, but featuring different substituents in the *para* position of the phenylpyridine (R = OH, F, Br, NO$_2$) (Fig. 2, **4**–**7**) in order to evaluate the effects of this ligand modification on the biological properties. Notably, complex **5** has already been described by Che et al. in 2013 as a precursor for photoactive functionalized bis-cyclometalated alkynyl gold(III) complexes suitable as phosphorescent organic light-emitting diodes (OLEDs).[19] However, the authors did not evaluate the biological activity of this complex. All the cyclometalated Au(III) complexes reported herein were studied for their antiproliferative effects against different human cancer cell lines, including some that are resistant to cisplatin. Moreover, compounds **1**–**3** were also tested for their inhibitory properties of TrxR on the purified protein and in cell lysates. The effects of the new complexes on the oxidation state of Trx were also investigated by Western blot analysis. Discrimination between the oxidation of the GSH/GSSG system and the Trx system can be very informative in terms of mechanisms of toxicity since different cellular pathways are controlled by GSH and Trx. Thus, estimation of the glutathione content was performed in treated cells.

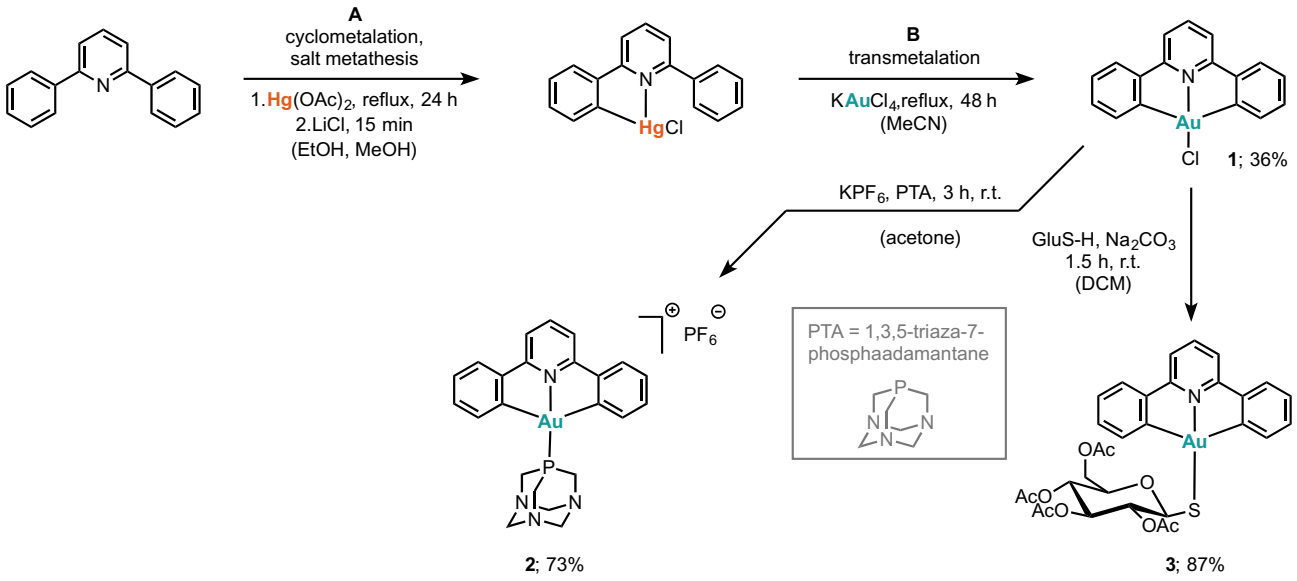

Fig. 2. General synthesis scheme of the obtained cyclometalated Au(III) [C^N^C] complexes **1**–**3**.

2. Results and discussion

2.1. Synthesis and structural characterization

To achieve the synthesis of the new compounds, the transmetalation pathway via the respective Hg(II) precursor was followed as described in Fig. 2. Thus, treatment of 2,6-diphenylpyridine or *para* substituted 2,4,6-triarylpyridines with mercury(II) acetate, followed by salt metathesis with LiCl, affords the organomercury(II) precursors (see Supplementary material for Hg complexes characterization, Figs. S16–S24). Subsequent transmetalation with K[$AuCl_4$] in refluxing acetonitrile, adapting previously reported procedures,[20] yields the respective cyclometalated Au(III) complexes. The synthesis of the cyclometalated precursor [Au(C^N^C)Cl] (C^N^C = 2,6-diphenylpyridine) (**1**) has been reported in 1998 by Che et al.,[20a] but the biological activity of this complex has not been reported. Afterwards, two novel derivatives, namely the cationic [Au(C^N^C)(PTA)][PF_6] (**2**) and the neutral [Au(C^N^C)(GluS)] (**3**), have been obtained from complex **1** by ligand exchange reactions (Fig. 2) and characterized by means of NMR, ESI-MS and elemental analysis.

Complex **2** contains the water-soluble ligand PTA, which, together with the positive charge of the resulting complex, should improve the overall water solubility while being non-cytotoxic *per se*. As has been reported before, replacement of a *trans* bound chlorido ligand by a tertiary phosphine at the Au(III) center can be achieved by first abstracting the halide to unveil a cationic gold (III) that can then be intercepted by the donor PTA ligand.[10,18]

Thus, by reacting **1** with one equivalent of PTA in the presence of KPF_6 in acetone for 3 h at room temperature, complex **2** is obtained in good yields. Single crystals of complex **2** suitable for X-ray diffraction were grown by slow diffusion of *n*-pentane into an acetone solution of the compound. The crystallographic structure of **2** is depicted in Fig. 3. The Au(III) centre is coordinated in a slightly distorted square planar fashion by the C^N^C pincer ligand and PTA with bond lengths of Au1–C1 = 2.106(3) Å, Au1–N1 = 2.025(2) Å, Au1–C17 = 2.091(3) Å and Au1–*P*1 = 2.2707(7) Å which are comparable to literature-reported values for the Au(III)-C^N^C[19] scaffold and an Au(III) ion binding to PTA.[10,21] While there is no significant out-of-plane distortion of the square planar arrangement, the geometry of the pincer ligand causes an in-plane distortion illustrated by the C1–Au1–C17 angle of 160.8(1)°. The pincer ligand itself is close to perfect planarity with only the phenyl-side-arm containing C17 slightly being bent out of plane and the C1–C6 phenyl ring being bent even more slightly in the antipodal direction.

Fig. S1 in the supplementary material depicts the allocation of the signals for ^1H and ^{13}C NMR spectra of the complexes. When comparing the free 2,6-diphenylpyridine ligand to the obtained complexes **1**–**3**, a significant shift in the ^1H NMR spectrum for H_f can be observed (see Fig. S1 in the supplementary material for the allocation of the signals for ^1H and ^{13}C NMR spectra of the complexes), resulting from the strong de-shielding caused by the –I effect of the electron-accepting Au-Cl moiety ($\Delta\delta$ = 0.48 ppm for complex **1**).

Complex **1** was also treated with one equivalent of thio-*β*-D-glucose tetraacetate (GluSH) and sodium carbonate in dichloromethane for 1.5 h at room temperature to obtain compound **3** in good yields. As this ligand is optically active, the ^1H NMR presents less sharp signals than the spectrum for complex **2**. The proton count, however, fits the structure of **3** perfectly and the signal of the thiol proton at 2.20 ppm is not present in the product NMR spectrum, confirming the bond formation between gold and sulfur, while the four acetate groups of the $GluS^-$ ligand appear as sharp singlet signals between 1.96 and 1.77 ppm. Moreover, all protons of the $GluS^-$ are shifted as well, resulting from the strong de-shielding caused by the –I effect of the electron-accepting Au(III) centre. The structure of complex **3** was further assessed by ESI-MS and elemental analysis.

Microwave assisted synthesis can afford several benefits, especially to modular synthesis programmes such as those concerning medicinal chemistry. Such benefits may come in the form of increased product purity and reduced reaction times.[22] The use of robotic handlers and touch-screen interfaces can greatly streamline the preparation of a library of compounds, especially when using an Initiator Robot system. Thus, the *para*-substituted 2,4,6-triaryl [$C^N^{R}^C$] ligands (L**4-7**) for complexes **4**–**7** (Fig. 4) were obtained by applying microwave assisted ligand synthesis. In detail, microwave irradiated synthesis of the [$C^N^{R}^C$] ligands was carried out adapting a previously reported procedure for hydroxylated tri-substituted pyridines.[23] Optimization of the reaction conditions was performed with respect to temperature, power

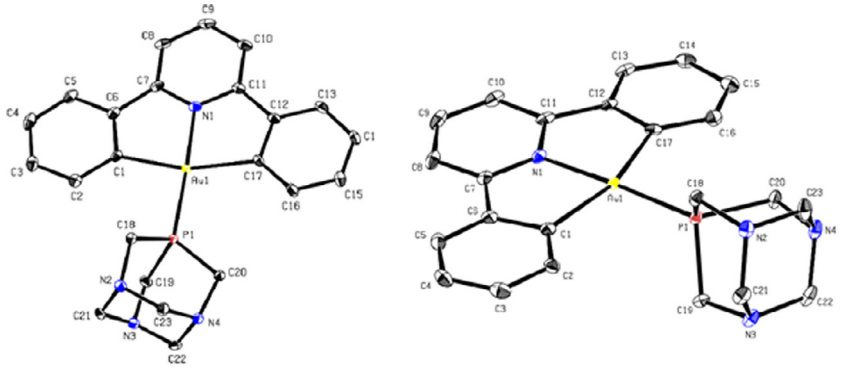

Fig. 3. ORTEP style presentation of the molecular structure of compound **2** in the solid state with ellipsoids given at 50% probability level. Hydrogen atoms, hexafluorophosphate anions and co-crystallized water molecules are omitted for clarity. Selected bond lengths (Å) and angles (°): Au1–C1 2.106(3), Au1–N1 2.025(2), Au1–C17 2.091(3), Au1–P1 2.2707(7), P1–Au1–C1 97.13(7), P1–Au1–C17 102.10(7), N1–Au1–C1 80.32(9), N1–Au1–C17 80.44(9).

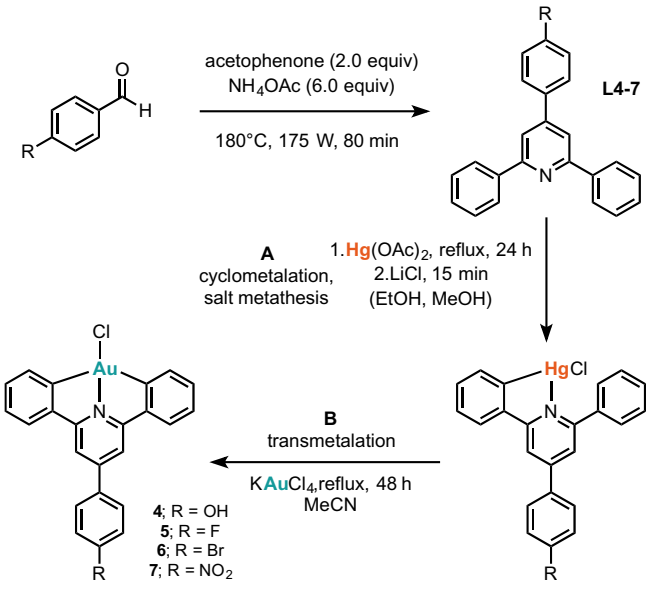

Fig. 4. Synthesis of [Au(III)(C^N^R^C)] (C^N^R^C = *para*-substituted 2,4,6-triarylpyridine) complexes.

and reaction time of the irradiation. A major benefit of the microwave synthesis is the circumvention of otherwise needed catalyst, such as previously reported $Bi(OTf)_3$,[24] and solvents, thus enabling a metal and solvent free synthesis.

A previously described procedure reports on the use of a conventional microwave with unfocused irradiation at 400 W.[23] We found this high power in our focussed reactor to cause pressure build up within in the system, leading to the termination of the microwave through triggering of the inbuilt safety features. A basis set (100 W, 120 °C, 30 min) was chosen, from which on the single parameters were optimized. The irradiation power has been altered as shown in Table S1 in the supplementary material, with the other parameters being fixed at basic conditions. The maximum product yield was found for a power of 175 W. The yield performance drops significantly after the power exceeds 200 W, which is believed to be contributed to beginning decomposition of the formed triarylpyridines.

The next parameter that could be altered is the temperature as depicted in Table S2 in the supplementary material. The maximum product yield was found for a temperature of 180 °C, while yield performance dropped significantly after the temperature exceeds 200 °C. The reaction time was the last parameter of the basis set to be altered as can be seen in Table S3. As expected, the yield reaches a plateau after a defined period of time (80 min and upwards). Overall, the combined optimized parameters for the microwave irradiated synthesis of the 2,4,6-triarylpyridine ligands were found to be at 180 °C, 175 W and 80 min.

Following the successful development of a microwave protocol for the preparation of the ligands, the cyclometalated Au(III) complexes were obtained via transmetalation of the respective [Hg(C^N^R^C)Cl] precursors with K[$AuCl_4$]. This was achieved by heating the reaction mixture to reflux in acetonitrile for 24 h (Fig. 4). Likewise, to the 2,6-diphenylpyridine systems, a significant shift in the ^{1}H NMR spectrum for H_1 can be observed when comparing the free 2,4,6-triaryl ligands to their respective complexes **4**–**7**, resulting from the strong de-shielding caused by the –I effect of the electron-accepting Au-Cl moiety ($\Delta\delta$ = 0.39 ppm for complex **4**).

The UV–visible absorption of complex **1** has been previously reported and shows a characteristic absorption with bands between 300 and 400 nm,[12] which were tentatively assigned to a metal-perturbed intraligand (IL) transition. We have obtained similar results in the case of complex **3**, whose UV–vis spectra have been recorded in PBS (pH 7.4) over 24 h (Fig. S25).

2.2. Antiproliferative activity

The gold complexes were tested for their cytotoxic activity against human cancer cell lines A549 (lung adenocarcinoma) SKOV-3 (ovarian adenocarcinoma) and 2008 (ovarian cancer), in comparison to their ligands, using a classical MTT assay as reported in the Experimental section. It is worth mentioning that A549 and SKOV-3 cells were chosen since they manifest resistance to cisplatin treatment. Overall, compounds **4**–**7** show modest activity in both A549 and SKOV-3 cell lines, with IC_{50} values >50 μM (Table 1). Similarly, the ligands **L4-L7** show very moderate effects. The highest antiproliferative effects are found for complexes **1** and **3** in 2008 cells, with IC_{50} values of 29 μM ± 3 and 7.0 μM ± 1.2, respectively.

2.3. Thioredoxin reductase inhibition

Since TrxR is also a potential target for gold complexes, *in vitro* inhibition of purified rat liver cytosolic and mitochondrial TrxR by compounds **1**–**3** was studied and compared with the activity of auranofin, a well-known TrxR inhibitor, using established protocols as described in the Experimental section. The results are summarized in Table 2. All compounds are good inhibitors of cytosolic thioredoxin reductase (TrxR1), showing IC_{50} values in

Table 1
IC_{50} values (μM) of the Au(III) compounds **1**–**7**, ligands (**L4-L7**) and cisplatin against A549 and SKOV-3 (72 h incubation) and 2008 (48 h incubation) cells.

compound	A549	SKOV-3	2008
1	35 ± 5	39 ± 7	29 ± 3
2	>50	48.1 ± 2.3	>50
3	30.4 ± 1.3	13.0 ± 0.9	7.0 ± 1.2
4	>50	>50	–
5	>50	>50	–
6	>50	>50	–
7	>50	>50	–
L4	30.0 ± 4.7	28.8 ± 5.5	–
L5	42.3 ± 5.3	44.5 ± 7.9	–
L6	30.8 ± 4.5	59.5 ± 9.7	–
L7	>100	>100	–
Cisplatin	12 ± 0.5	16.3 ± 1.7	10.3 ± 1.4

the nanomolar range of concentrations, with complex **3** being the most potent. Conversely, the mitochondrial isoform of the enzyme is slightly inhibited by the three complexes after incubation in the same experimental conditions, revealing a different inhibitory capacity on the two isoforms. Further studies demonstrated that **3** is also able to inhibit the TrxR closely related, but selenium-free, enzyme glutathione reductase (GR) although 60-fold less efficiently than in the case of TrxR (Table 2).

The effect of compounds **1**–**3** on TrxR and GR activities was also evaluated in cell lysates. For this purpose, 2008 cells, where the three compounds showed markedly different cytotoxic effects, were pre-treated for 48 h with **1**–**3** at different concentrations (Fig. 5). Complex **3** was the most effective in inhibiting TrxR, followed by compound **2**. Complex **1** was scarcely active. In addition, GR activity was also determined and, as shown in the insert of Fig. 5, the enzyme was not inhibited by the compounds even at 50 μM concentration.

2.4. Effects on cellular redox state

Furthermore, the cellular redox state was evaluated after the incubation of 2008 cells with **1**–**3**. For the determination of the total thiols in cell lysates, an assay was conducted according to the protocol described in the Experimental section. The results presented in Fig. 6A show that the total amount of thiols is unaltered upon treatment with **1** and **2**, indicating that these complexes have no effect on the redox state of the intracellular sulfhydryl groups, while at 50 μM, **3** shows a decrease of about 40% of the total thiols. This suggests that **3** determines a redox imbalance interacting with thiols inside the cells.

Since the glutathione redox pair (GSH/GSSG) is another fundamental indicator of the cell redox state, an analysis of the total glutathione content and of the GSH/GSSG ratio was performed in 2008 cells, after treatment with **1**–**3** for 48 h. The obtained results are elucidated in Fig. 6B. After the treatment of 5×10^5 ovarian cancer cells, an important increase of oxidized glutathione, suggesting thiols oxidation, can be observed only in the presence of **3** (50 μM), while **1** and **2** do not affect the glutathione system since total and oxidized levels were comparable to the control cells (Fig. 6B).

Table 2
IC_{50} values of the inhibition of TrxR1, TrxR2 and GR on the isolated enzymes.

Complex	IC_{50} (nM)		
	TrxR1	TrxR2	GR
Auranofin	0.9 ± 0.3	3 ± 1	>10,000
1	10 ± 1	59 ± 5	219 ± 18
2	10 ± 1	213 ± 20	439 ± 7
3	3 ± 1	60 ± 4	180 ± 22

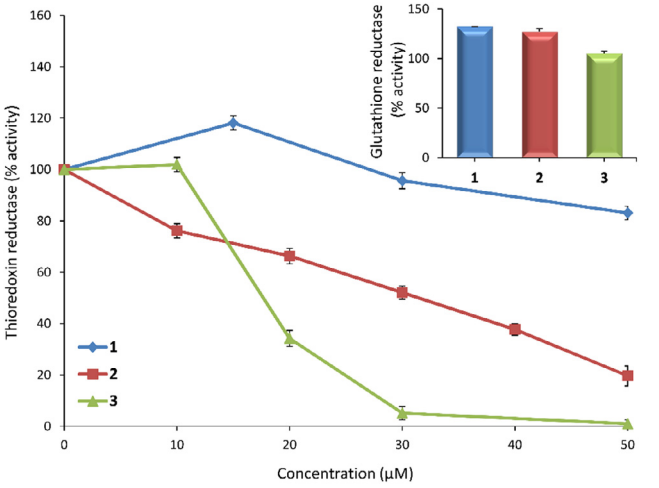

Fig. 5. Thioredoxin reductase and glutathione reductase (insert) activities in 2008 ovarian cancer cells after 48 h treatment with **1**–**3**. For TrxR activity determinations, cells (1×10^6) were treated with the compounds at the indicated concentrations. GR activity was evaluated after cells treatment with 50 μM of each of the three compounds, as reported in the Experimental section.

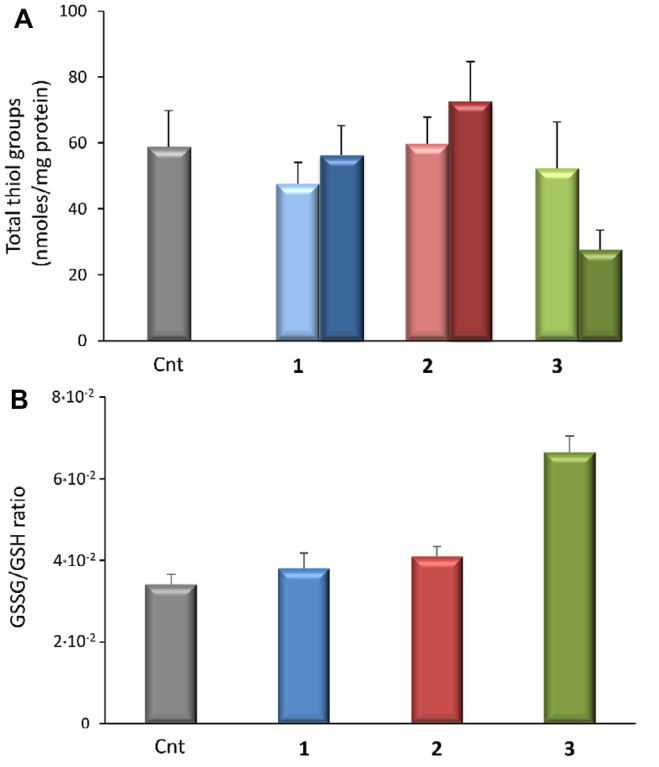

Fig. 6. (A) Total thiols in 2008 ovarian cancer cells after treatment with **1**–**3**. Cells (5×10^5) were treated with the compounds at the indicated concentrations and then subjected to total thiol determination (light bars: 25 μM; dark bars: 50 μM). (B) Glutathione redox state ratio (GSSG/GSH) after cell treatment with 50 μM of the three compounds.

Therefore, the redox state of Trx1 and Trx2 in 2008 cells treated for 48 h with **1** and **3** was studied (Fig. S26, supplementary material) to confirm that the inhibition of TrxR determines an increase of oxidation of the principal substrates. Interestingly, complex **3** induces a marked oxidation of Trx1 and Trx2, evidenced by the shift of the bands relative to the two proteins towards their oxidized form by western-blot analysis, providing indirect evidence that TrxR is a pivotal target of this compound in cells.

3. Conclusions

Two new Au(III)[C^N^C] complexes, [Au(C^N^C)(PTA)][PF_6] (**2**) and [Au(C^N^C)(GluS)] (**3**), and three new Au(III)[C^N(R)^C] complexes with R = Ph-*p*-OH (**4**), Ph-*p*-Br (**6**), Ph-*p*-NO_2 (**7**) have been synthesized. Microwave assisted ligand synthesis for the *para* substituted 2,4,6-triaryl ligands for complex **4**–**7** was optimized concerning applied temperature, power and reaction time. The compounds have been examined for their antiproliferative effects in a small panel of human cancer cells. In general, the compounds are poorly toxic, with the exception of compounds **1** and **3**, which were active in the 2008 ovarian cancer cells. Initial mechanistic studies have shown that **1**–**3** are nanomolar inhibitors of isolated cytosolic and mitochondrial TrxRs, while they scarcely affect the activity of GR, supporting the idea that they could bind preferentially TrxRs. These results are confirmed also in an ovarian cancer cell line and supported by the observed increase of the oxidized form of Trxs, upon metallodrugs' treatment. Furthermore, the observed effects of complex **3** on the overall cellular redox state suggest that this derivative is particularly effective in disrupting the thiol redox homeostasis of the cell. Overall, the obtained results demonstrate that the reported Au(III) complexes need to be further optimized for biological applications, especially in terms of solubility and potency on cancer cells. Moreover, a central role of the ancillary ligands in the observed anticancer effects has been highlighted, in line with previous studies by Che et al. Nevertheless, these initial results provide some indications on the possible cellular targets for this family of compounds.

In terms of possible derivatization of the organometallic scaffold, Au(C^N^C) systems replacing the central pyridine ring with a pyrazine have been reported recently.[25] As they display intense thermally activated delayed fluorescence (TADF), these Au(C^N^C) complexes could lead to a convenient way to monitor the uptake of anticancer compounds via fluorescence microscopy.

4. Experimental section

4.1. General remarks

Reactions were carried out under purified argon using standard Schlenk techniques. Solvents were dried, degassed and stored over molecular sieve and under argon before use. Microwave reactions were carried out in a CEM Focused Microwave™ Synthesis System or a Biotage® Initiator Robot Eight and Sixty. All physico-chemical analytics were performed at the Technische Universität München and the University of Cardiff. UV−vis spectra were recorded on a Perkin-Elmer Lambda 650 UV/vis spectrophotometer. Electrospray ionization mass spectra (ESI-MS) were obtained on a High-Resolution Waters LCT TOF Bruker HR-QTOF maXisPlus operating in positive ionization mode. The samples were dissolved in 1 ml of the appropriate solvent and 10 μl were injected directly into the mass spectrometer. The mass range was scanned between 100 and 2000 and Leucine Enkephalin was used as an online calibrant. NMR spectra were recorded on a Bruker Avance DPX-300, 400 or 500 at 298 K. All deuterated solvents were purchased from Deutero GmbH and Sigma Aldrich. Chemical shifts are given in δ (ppm) and refer to the residual ^{1}H and ^{13}C(^{1}H) signals of the respective solvent. In allocating the signals the following abbreviations have been used: s- singlet, d- doublet, t -triplet, q-quartet, m- multiplet. Coupling constants *J* are given in Hz. X-ray intensity data were measured on a Bruker D8 Venture Duo IMS system equipped with a Helios optic monochromator and a Mo IMS microsource (λ = 0.71073 Å). All mercury precursors were prepared according to Constable et al.[20b] The commercially available ligand 2,6-diphenylpyridine (CAS 3558-69-8) and Au(III) precursor K[$AuCl_4$] (98%, CAS 13682-61-6) were purchased from Sigma-Aldrich and utilized without further purification. Crystallographic Details are reported in the Supporting Information.

4.2. Synthesis of [Au(III)(C^N^C)]$^{n+}$ (C^N^C = 2,6-diphenylpyridine) complexes

4.2.1. [Au(C^N^C)Cl] (*1*)

Preparation was carried out with slight changes to the synthesis by Che et al.[20a]

Hg(C^N^CH)Cl (1 eq, 0.51 g, 1.09 mmol) and K[$AuCl_4$] (1 eq, 0.41 g, 1.09 mmol) are refluxed in acetonitrile (20 mL) under argon for 24 h at 80°C forming a greenish precipitate. The crude solid is filtered, washed with diethyl ether and *n*-pentane and dried under reduced pressure to afford an electrostatic light-yellow, solid (0.18 g, 0.39 mmol, 36% yield). ^{13}C NMR spectra have not been reported in the literature so far.

^{1}H NMR (400 MHz, DMSO-d_6) δ 8.19 (t, *J* = 8.0 Hz, 1H, H_a), 7.98 (d, *J* = 8.1 Hz, 2H, H_f), 7.88 (d, *J* = 7.7 Hz, 2H, H_c), 7.69 (d, *J* = 7.2 Hz, 2H, H_b), 7.43 (t, *J* = 7.3 Hz, 2H, H_d), 7.32 (t, *J* = 7.6 Hz, 2H, H_e). ^{13}C (^{1}H) NMR (101 MHz, DMSO) δ 169.5 (C-N), 164.1 (C–C), 148.4 (C-H_a), 142.3 (C-Au), 133.0 (C-H_c), 131.7 (C-H_e), 127.6 (C-H_d), 126.1 (C-H_f), 118.6 (C-H_b). Positive ESI-MS (acetone): *m*/*z* = 462.21 [M+H]$^+$ (calcd for $C_{17}H_{12}AuClN$: 462.03). Anal. Calc. for $C_{17}H_{11}AuClN$: C, 44.22; H, 2.40; N, 3.03%. Found: C, 44.16; H, 2.18; N, 3.23%.

4.2.2. [Au(C^N^C)(PTA)][PF_6] (*2*)

Complex **1** (1 eq., 100 mg, 0.22 mmol) is added to KPF_6 (5 eq., 202.47 mg, 1.10 mmol) in acetone (25 mL). PTA (1 eq., 34.57 mg, 0.22 mmol) is added to the suspension at room temperature under vigorous stirring. The reaction is stirred at room temperature for 3 h. Acetone is subsequently partly removed, dichloromethane was added and the solution was filtered through Celite®. The volatiles are removed under reduced pressure and the resulting white solid is washed with ice-cold acetone, *n*-pentane and diethylether (114.7 mg, 0.16 mmol, 73% yield).

^{1}H NMR (400 MHz, Acetone-d_6) δ 8.28 (t, *J* = 8.0 Hz, 1H, H_a), 8.01 (m, *J* = 8.5 Hz, 6H, $H_{b,c,f}$), 7.56 (t, *J* = 7.5 Hz, 2H, H_d), 7.46 (t, *J* = 7.5 Hz, 2H, H_e), 5.21 (d, *J* = 2.1 Hz, 6H, N-CH_2), 4.99 (d, *J* = 13.1 Hz, 3H, P-CH_aH_b), 4.80 (d, *J* = 13.3 Hz, 3H, P-CH_aH_b). ^{13}C NMR (101 MHz, Acetone-d_6) δ 169.5 (C-N), 164.7 (C-C), 151.4 (C-H_a), 146.4 (C-Au), 137.6 (C-H_c), 133.5 (C-H_e), 129.1 (C-H_d), 128.0 (C-H_f), 119.6 (C-H_b), 73.1 (N-CH_2), 51.3 (P-CH_2). Positive ESI-MS (acetone): *m*/*z* = 583.110 [M]$^+$ (calcd for $C_{23}H_{23}AuN_4P$: 583.126). Anal. Calc. for $C_{23}H_{23}AuF_6N_4P_2$: C, 37.93; H, 3.18; N, 7.69%. Found: C, 37.79; H, 3.24; N, 7.38%.

4.2.3. [Au(C^N^C)(GluS)] (*3*)

Complex **1** (1 eq., 50 mg, 0.115 mmol), is added to thio-β-D-glucose tetraacetate (1 eq., 41.9 mg, 0.115 mmol) and Na_2CO_3 (5 eq., 61 mg, 0.575 mmol) in dichloromethane (20 mL). The suspension is stirred for 1.5 h at room temperature. The solution is filtered through Celite® and concentrated under reduced pressure. Upon cooling and subsequent addition of pentane a light yellow precipitate is formed which is filtered, washed with diethylether and *n*-pentane and dried under reduced pressure (78.96 mg, 0.10 mmol, 87% yield).

^{1}H NMR (500 MHz, Acetone-d6) δ 8.34–7.69 (m, 5H, $H_{a,b,c}$), 7.61–7.14 (m, 6H, $H_{d,e,f}$), 5.20–5.10 (m, 2H, 2 CH), 4.98 (m, 1H, CH), 4.89 (t, *J* = 9.4 Hz, 1H, CH), 4.79 (t, *J* = 9.7 Hz, 1H, CH), 4.15 (dd, *J* = 12.3 Hz, 2.1 Hz, 1H, CH_2-sugar), 4.02 (dd, *J* = 12.3 Hz, 5.6 Hz, 1H, CH_2-sugar), 1.96 (s, 3H, OAc), 1.94 (s, 3H, OAc), 1.86 (s, 3H, OAc), 1.77 (s, 3H, OAc). Positive ESI-MS (acetone): *m*/*z* = 790.1442 [M+H]$^+$ (calcd for $C_{31}H_{31}AuNO_9S$: 790.1385). Anal. Calc. for $C_{31}H_{30}AuNO_9S$: C, 47.15; H 3.83; N, 1.77; S, 4.06%. Found: C, 47.01; H, 3.68; N, 1.85; S, 3.75%.

4.3. Synthesis of [Au(III)(C^NR^C)] (C^NR^C = substituted 2,4,6-triarylpyridine) complexes

4.3.1. General procedure

*4.3.1.1. C^NR^C ligand synthesis (**L1**–**L7**).* A mixture of the respective *para*-substituted benzaldehyde (1 eq), acetophenone (2.0 eq) and ammonium acetate (6.0 eq) is subjected to microwave irradiation of 180 W at 175 °C for 80 min. The resulting biphasic reaction mixture is then transferred to a separating funnel, treated with equal volumes of ice-water and diethyl ether and shaken well. The aqueous phase containing excess ammonium acetate is extracted three times with diethyl ether. The organic phases are combined and concentrated under reduced pressure to afford the crude product. Recrystallization from ethanol and subsequent drying under reduced pressure delivers the respective C^N(R)^C ligand. Column chromatography over silica gel (hexane/ethyl acetate = 1.5/1) can be performed if required.

4.3.1.2. [Au(III)(C^NR^C)] complex synthesis. The respective Hg(C^N^{R}^CH)Cl precursor (1 eq, 100 μmol) and K[$AuCl_4$] (1 eq, 100 μmol) are added to acetonitrile (20 mL) using standard Schlenk techniques. Under vigorous stirring the suspension is kept at 100 °C for 48 h under reflux upon which solubilisation of the educts occurs. The solution is then allowed to cool to room temperature leading to the precipitation of a solid. The crude product is filtered and then washed with ice-cold diethyl ether and *n*-pentane. Any remaining solvent is removed under reduced pressure to afford the complexes as solids.

*4.3.1.2.1. [Au(III)(C^N^{OH}^C)Cl] (**1**).* The compound is obtained as a pale yellow solid (38,77 mg, 70 μmol, 70% yield). ^{1}H NMR (400 MHz, DMSO-d_6) δ 9.76 (s, 1H, OH), 8.27 (d, J = 6.8 Hz, 4H, $H_{1,4}$), 8.06 (d, J = 13.7 Hz, 4H, $H_{6,7}$), 7.60–7.53 (m, 4H, $H_{2,3}$), 7.51–7.46 (m, 2H, H_5). ^{13}C NMR (101 MHz, $CDCl_3$) δ 157.5 (2C-N), 151.2 (C-OH), 150.0 (C_{para}-N), 140.1 (C-Au), 129.0, 128.9, 128.8, 128.0, 127.3, 127.3, 126.2, 116.8, 116.2, 112.6. Positive ESI-MS (acetone/water): m/z = 571.0382 $[M+H_2O]^+$ (calcd for $C_{23}H_{17}AuClNO_2$: 571.0613). Anal. Calc. for $C_{23}H_{15}AuClNO$: C, 49.88; H, 2.73; N, 2.53%. Found: C, 49.63; H, 2.55; N, 2.57%.

*4.3.1.2.2. [Au(III)(C^N^{F}^C)Cl] (**2**).* The compound is obtained as a pale yellow solid (35.01 mg, 63 μmol, 63% yield). ^{1}H NMR (300 MHz, DMSO-d_6) δ 8.32 (s, 2H, H_5), 8.25 (m, 2H, H_7), 8.12 (d, J = 7.7 Hz, 2H, H_4), 7.70 (d, J = 7.2 Hz, 2H, H_1), 7.54–7.41 (m, 4H, $H_{2,3}$), 7.34 (m, 2H, H_6). ^{13}C NMR (101 MHz, DMSO) δ 189.1 (C-F), 142.7 (C-Au), 137.4 (2 C-N), 134.0 (C_{para}-N), 133.3, 131.9, 131.3, 130.9, 128.9, 128.6, 128.1, 124.1, 122.8. Positive ESI-MS (acetone): m/z = 555.0463 $[M]^+$ (calcd for $C_{23}H_{17}AuClNO_2$: 555.0464). Anal. Calc. for $C_{23}H_{14}AuClFN$: C, 47.15; H 3.83; N, 1.77%. Found: C, 47.04; H 3.68; N, 1.79%.

*4.3.1.2.3. [Au(III)(C^N^{Br}^C)Cl] (**3**).* The compound is obtained as a pale yellow solid (40.08 mg, 65 μmol, 65% yield). ^{1}H NMR (300 MHz, DMSO-d_6) δ 8.32 (s, 2H, H_5), 8.12 (m, 4H, $H_{4,1}$), 7.85 (d, J = 6.0 Hz, 2H, H_7), 7.71 (d, J = 8.0 Hz, 2H, H_6), 7.50–7.41 (m, 2H, H_2), 7.40–7.29 (m, 2H, H_3). ^{13}C NMR (75 MHz, DMSO) δ 157.1 (2 C-N), 148.8 (C_{para}-N), 139.1 (C-Au), 137.3, 132.4, 130.0, 129.8, 129.2, 127.4 (C-Br), 124.4, 117.0. Positive ESI-MS (acetone): m/z = 616.9659 $[M]^+$ (calcd for $C_{23}H_{17}AuClNO_2$: 614.9664). Anal. Calc. for $C_{23}H_{14}AuBrClN$: C, 44.80; H, 2.29; N, 2.27%. Found: C, 44.61; H, 2.24; N, 2.36%.

*4.3.1.2.4. [Au(III)(C^N^{NO2}^C)Cl] (**4**).* The compound is obtained as a pale yellow solid (35.55 mg, 61 μmol, 61% yield). ^{1}H NMR (400 MHz, DMSO-d_6) δ 8.44 (s, 2H, H_5), 8.32 (d, J = 8.6 Hz, 2H, H_7), 8.23 (d, J = 8.7 Hz, 2H, H_6), 7.87–7.74 (m, 4H, $H_{1,4}$), 7.58–7.51 (m, 2H, H_3), 7.50–7.40 (m, 2H, H_2). ^{13}C NMR (75 MHz, DMSO) δ 157.2 (2 C-N), 148.3 (C-NO_2), 147.8 (C_{para}-N), 144.6, 144.1, 138.9 (C-Au), 130.0, 129.9, 129.3, 129.2, 127.5, 124.5, 117.4. Positive ESI-MS (acetone): m/z = 582.0400 $[M]^+$ (calcd for $C_{23}H_{17}AuClNO_2$: 582.0409). Anal. Calc. for $C_{23}H_{14}AuClN_2O_2$: C, 47.40; H, 2.42; N, 4.81%. Found: C, 47.34; H, 2.37; N, 4.83%.

4.4. Antiproliferative assays

The human cancer cell lines A549 (lung adenocarcinoma) and SKOV-3 (ovarian adenocarcinoma) were cultured in DMEM containing GlutaMax-I supplemented with 10% FBS and 1% penicillin/streptomycin, at 37 °C in a humidified atmosphere of 95% of air and 5% CO_2, while 2008 ovarian cancer cells were grown in RPMI with 10% FBS, 2 mM glutamine and 1% penicillin/streptomycin in the same conditions. Cells in an exponential growth rate were seeded in 96-well plates) at a concentration of 8×10^3 cells/well, and grown for 24 h in complete medium. Solutions of the compounds were prepared by diluting a stock solution in DMSO (10^{-2} M) of the corresponding compound in culture media (the percentage of DMSO in the culture medium never exceeded 0.5%). Cisplatin was dissolved in aqueous solution (10^{-3} M) to avoid ligand exchange reactions with DMSO. Subsequently, intermediate dilutions of the compounds were added to the wells to obtain a final concentration ranging from 0.5 to 100 μM. Following 72 h (A549, SKOV-3) or 48 h (2008) drug exposure, medium was removed and 3 (4,5-dimethylthiazol-2-yl)-2,5-diphenyltetrazolium bromide (MTT) in PBS/10 mM glucose was added to the cells at a final concentration of 0.50 mg/mL and incubated for 2.5 h. Afterwards, the medium was removed and the violet formazan crystals dissolved in DMSO. The optical density of each treatment was quantified in quadruplicate at 540 nm, using a multi-well plate reader (ThermoMax microplate reader, Molecular devices, US), and the percentage of surviving cells was calculated from the ratio of absorbance between treated and untreated cells. The IC_{50} value was calculated as the concentration reducing the proliferation of the cells by 50% and is presented as a mean (±SD) of at least three independent experiments.

4.5. Inhibition assays on isolated enzymes

Highly purified aliquots of cytosolic and mitochondrial rat liver thioredoxin reductases[26,27] were utilized. Thioredoxin reductases activity was determined in 0.2 M NaKPi buffer, 5 mM EDTA, pH 7.4, by estimating the DTNB reduction in the presence of 0.25 mM NADPH after 5 min incubation with increasing concentration of **1**–**3**. The reaction was started with 1 mM DTNB and followed spectrophotometrically at 412 nm for about 10 min at 25 °C on a Lambda 2 spectrophotometer (Perkin-Elmer, Waltham, Massachusetts, USA). Yeast glutathione reductase activity was measured in 0.2 M Tris–HCl buffer (pH 8.1), 1 mM EDTA, and 0.25 mM NADPH, with the various compounds. The assay was initiated by addition of 1 mM GSSG and followed spectrophotometrically at 340 nm.

4.6. Analysis of thioredoxin reductase and glutathione reductase activities in cell lysates

2008 ovarian cancer cells (1×10^6) were incubated with increasing concentrations of the three compounds for 48 h. Then, cells were harvested, washed with PBS and lysed with a modified RIPA buffer: 150 mM NaCl, 50 mM Tris-HCl, 1 mM EDTA, 0.1% SDS, 0.5% DOC, 1 mM NaF, supplemented with an antiprotease cocktail ("Complete" Roche, Mannheim, Germany) and 0.1 mM PMSF. After 40 min of incubation at 4 °C, lysates were centrifuged at 14,000*g* for 5 min and aliquots (50 μg) of the supernatants were utilized for enzyme activities as described in the previous paragraph.

4.7. Total thiols estimation in 2008 cell lysates

After treatment with 25 or 50 μM of the gold compounds for 24 h, cells were washed in PBS and dissolved with 7.2 M guanidine in a buffer containing 0.2 M Tris-HCl, 5 mM EDTA, pH 8.1. Then, 3 mM DTNB was added to titrate the free thiol groups and the absorbance increase was monitored at 412 nm for 5 min.

4.8. Total and oxidized glutathione evaluation in cell lysates

First, 5×10^5 2008 cells, were incubated for 48 h with 50 μM of **1**–**3**. Then cells, washed twice with cold PBS, were rapidly lysed and deproteinized with 6% *meta*-phosphoric acid. After 10 min at 4 °C, samples were centrifuged and supernatants were neutralized with 15% Na_3PO_4 and assayed for total glutathione, essentially as described in Ref. 28.

To determine the amount of GSSG, aliquots (0.2 mL) of the obtained samples were derivatized with 2-vinylpyridine in order to block reduced glutathione, and oxidized glutathione was then estimated.[29]

4.9. Redox Western blot analysis of Trx1 and Trx2

The redox state of Trx1 and 2 was detected using a modified Western blot analysis[30] utilizing the protocol describe in Ref. 31. Briefly, 2008 ovarian cancer cells (5×10^5) incubated with the compounds for 48 h, were lysed with 150 μL of urea lysis buffer (100 mM Tris-HCl, pH 8.3) containing 1 mM EDTA, 8 M urea supplemented with 10 mM iodoacetamide (IAM) to derivatize free thiols. The incubation was carried out for 20 min at 37 °C. Subsequently, after the treatment with 3.5 mM DTT for 30 min at 37 °C to reduce the oxidized thiols, cell lysates were derivatized with iodoacetic acid (IAA) (30 mM final concentration) for 30 min at 37 °C. Proteins (0.01 mg) were separated by urea-PAGE gel (7% acrylamide/bis(acrylamide) in 7 M urea) in non-reducing conditions and blotted using Transblot Turbo transfer system (Bio-Rad Laboratories, Hercules, CA, USA). Membranes were probed with the primary antibodies for Trx1 (FL 105) and for Trx2 (H75) (Santa Cruz Biotechnology, Santa Cruz, CA, USA) respectively.

Acknowledgements

Authors thank Cardiff University and Technische Universität München (TUM) Graduate School for funding, as well as the Department of Sciences, Technology, and Innovation COLCIENCIAS (Colombia) for a fellowship to N.E.O. A.C. acknowledges a Hans Fischer Senior Fellowship of the TUM – Institute for Advanced Study, funded by the German Excellence Initiative and the European Union Seventh Framework Programme under grant agreement n° 291763. Authors acknowledge Dr Alexander Pöthig's support with crystallographic data analysis. M.P.R thanks the Consorzio Interuniversitario di Ricerca in Chimica dei Metalli nei Sistemi Biologici (CIRCSMB).

A. Supplementary data

Supplementary data associated with this article can be found, in the online version, at http://dx.doi.org/10.1016/j.bmc.2017.08.001.

References

1. (a) Cinellu M, Ott I, Casini A. Gold Organometallics with Biological Properties. In: Gérad Jaouen MS, ed. *Bioorganometallic Chemistry: Applications in Drug Discovery, Biocatalysis, and Imaging*. First Edition ed. Wiley-VCH Verlag GmbH & Co. KGaA; 2015:117–139;
(b) Zou T, Lum CT, Lok C-N, Zhang J-J, Che C-M. Chemical biology of anticancer gold (III) and gold (I) complexes. *Chem Soc Rev*. 2015;44:8786–8801;
(c) Bertrand B, Casini A. A golden future in medicinal inorganic chemistry: the promise of anticancer gold organometallic compounds. *Dalton Trans*. 2014;43:4209–4219;
(d) Nobili S, Mini E, Landini I, Gabbiani C, Casini A, Messori L. Gold compounds as anticancer agents: chemistry, cellular pharmacology, and preclinical studies. *Med Res Rev*. 2010;30:550–580.
2. Gasser G, Ott I, Metzler-Nolte N. Organometallic Anticancer Compounds. *J Med Chem*. 2011;54:3–25.
3. (a) Schaper L-A, Hock SJ, Herrmann WA, Kühn FE. Synthesis and Application of Water-Soluble NHC Transition-Metal Complexes. *Angew Chem Int Ed*. 2013;52:270–289;
(b) Velazquez HD, Verpoort F. N-heterocyclic carbene transition metal complexes for catalysis in aqueous media. *Chem Soc Rev*. 2012;41:7032–7060.
4. (a) Meggers E. Targeting proteins with metal complexes. *Chem Commun*. 2009;9:1001–1010;
(b) Oehninger L, Rubbiani R, Ott I. N-Heterocyclic carbene metal complexes in medicinal chemistry. *Dalton Trans*. 2013;42:3269–3284;
(c) Jaouen G, Vessieres A, Top S. Ferrocifen type anti cancer drugs. *Chem Soc Rev*. 2015;44:8802–8817;
(d) Gautier A, Cisnetti F. Advances in metal–carbene complexes as potent anticancer agents. *Metallomics*. 2012;4:23–32;
(e) Mercs L, Albrecht M. Beyond catalysis: N-heterocyclic carbene complexes as components for medicinal, luminescent, and functional materials applications. *Chem Soc Rev*. 2010;39:1903–1912.
5. Hickey JL, Ruhayel RA, Barnard PJ, Baker MV, Berners-Price SJ, Filipovska A. Mitochondria-Targeted Chemotherapeutics: The Rational Design of Gold(I) N-Heterocyclic Carbene Complexes That Are Selectively Toxic to Cancer Cells and Target Protein Selenols in Preference to Thiols. *J Am Chem Soc*. 2008;130:12570–12571.
6. Muenzner JK, Rehm T, Biersack B, et al. Adjusting the DNA interaction and anticancer activity of Pt (II) N-heterocyclic carbene complexes by steric shielding of the trans leaving group. *J Med Chem*. 2015;58:6283–6292.
7. Cutillas N, Yellol GS, de Haro C, Vicente C, Rodríguez V, Ruiz J. Anticancer cyclometalated complexes of platinum group metals and gold. *Coord Chem Rev*. 2013;257:2784–2797.
8. Buckley RG, Elsome AM, Fricker SP, et al. Antitumor properties of some 2-[(dimethylamino) methyl] phenylgold (III) complexes. *J Med Chem*. 1996;39:5208–5214.
9. Cinellu MA, Zucca A, Stoccoro S, Minghetti G, Manassero M, Sansoni M. Synthesis and characterization of gold(III) adducts and cyclometallated derivatives with 6-benzyl- and 6-alkyl-2,2[prime or minute]-bipyridines. *J Chem Soc, Dalton Trans*. 1996;22:4217–4225.
10. Bertrand B, Spreckelmeyer S, Bodio E, et al. Exploring the potential of gold(iii) cyclometallated compounds as cytotoxic agents: variations on the C^N theme. *Dalton Trans*. 2015;44:11911–11918.
11. Gabbiani C, Casini A, Kelter G, et al. Mechanistic studies on two dinuclear organogold(III) compounds showing appreciable antiproliferative properties and a high redox stability. *Metallomics*. 2011;3:1318–1323.
12. Li CKL, Sun RWY, Kui SCF, Zhu N, Che CM. Anticancer cyclometalated [AuIIIm (C∧ N∧ C) mL] n+ compounds: synthesis and cytotoxic properties. *Chem Eur J*. 2006;12:5253–5266.
13. Yan JJ, Chow AL-F, Leung C-H, Sun RW-Y, Ma D-L, Che C-M. Cyclometalated gold (III) complexes with N-heterocyclic carbene ligands as topoisomerase I poisons. *Chem Commun*. 2010;46:3893–3895.
14. (a) Wai-Yin Sun R, Ma D-L, Wong EL-M, Che C-M. Some uses of transition metal complexes as anti-cancer and anti-HIV agents. *Dalton Trans*. 2007;43:4884–4892;
(b) Hsiang Y-H, Liu LF. Identification of mammalian DNA topoisomerase I as an intracellular target of the anticancer drug camptothecin. *Cancer Res*. 1988;48:1722–1726.
15. Zhang JJ, Lu W, Sun RWY, Che CM. Organogold (III) supramolecular polymers for anticancer treatment. *Angew Chem Int Ed*. 2012;51:4882–4886.
16. (a) de Almeida A, Oliveira BL, Correia JD, Soveral G, Casini A. Emerging protein targets for metal-based pharmaceutical agents: An update. *Coord Chem Rev*. 2013;257:2689–2704;
(b) Gabbiani C, Mastrobuoni G, Sorrentino F, et al. Thioredoxin reductase, an emerging target for anticancer metallodrugs. Enzyme inhibition by cytotoxic gold (III) compounds studied with combined mass spectrometry and biochemical assays. *MedChemComm*. 2011;2:50–54;
(c) Cinellu MA, Maiore L, Manassero M, et al. $[Au_2(phen_2Me)_2(\mu\text{-}O)_2](PF6)_2$, a novel dinuclear gold (III) complex showing excellent antiproliferative properties. *ACS Med Chem Lett*. 2010;1:336–339;
(d) Citta A, Scalcon V, Göbel P, et al. Toward anticancer gold-based compounds targeting PARP-1: a new case study. *RSC Adv*. 2016;6:79147–79152.
17. Bindoli A, Rigobello MP, Scutari G, Gabbiani C, Casini A, Messori L. Thioredoxin reductase: a target for gold compounds acting as potential anticancer drugs. *Coord Chem Rev*. 2009;253:1692–1707.
18. Cinellu MA. Synthesis and characterization of gold (III) adducts and cyclometallated derivatives with 6-benzyl-and 6-alkyl-2, 2′-bipyridines. *J Chem Soc, Dalton Trans*. 1996;22:4217–4225.
19. Au VK-M, Tsang DP-K, Wong KM-C, Chan M-Y, Zhu N, Yam VW-W. Functionalized bis-cyclometalated alkynylgold (III) complexes: synthesis, characterization, electrochemistry, photophysics, photochemistry, and electroluminescence studies. *Inorg Chem*. 2013;52:12713–12725.
20. (a) Wong K-H, Cheung K-K, Chan MC-W, Che C-M. Application of 2,6-diphenylpyridine as a tridentate [C^N^C] dianionic ligand in organogold (III)

chemistry. Structural and spectroscopic properties of mono-and binuclear transmetalated gold (III) complexes. *Organometallics*. 1998;17:3505–3511; (b) Constable EC, Leese TA. Metal exchange in organomercury complexes; a facile route to cyclometallated transition metal complexes. *J Organomet Chem*. 1987;335:293–299.
21. Fuchita Y, Ieda H, Tsunemune Y, Kinoshita-Nagaoka J, Kawano H. Synthesis, structure and reactivity of a new six-membered cycloaurated complex of 2-benzoylpyridine [$AuCl_2$(pcp-C_1,N)][pcp = 2-(2-pyridylcarbonyl)phenyl]. Comparison with the cycloaurated complex derived from 2-benzylpyridine. *J Chem Soc, Dalton Trans*. 1998;5:791–796.
22. Kappe CO. Controlled microwave heating in modern organic synthesis. *Angew Chem Int Ed*. 2004;43:6250–6284.
23. Yin G, Liu Q, Ma J, She N. Solvent-and catalyst-free synthesis of new hydroxylated trisubstituted pyridines under microwave irradiation. *Green Chem*. 2012;14:1796–1798.
24. Shinde PV, Labade VB, Gujar JB, Shingate BB, Shingare MS. Bismuth triflate catalyzed solvent-free synthesis of 2,4,6-triaryl pyridines and an unexpected selective acetalization of tetrazolo[1,5-*a*]-quinoline-4-carbaldehydes. *Tetrahedron Lett*. 2012;53:1523–1527.
25. Fernandez-Cestau J, Bertrand B, Blaya M, Jones GA, Penfold TJ, Bochmann M. Synthesis and luminescence modulation of pyrazine-based gold (III) pincer complexes. *Chem Commun*. 2015;51:16629–16632.
26. Luthman M, Holmgren A. Rat liver thioredoxin and thioredoxin reductase: purification and characterization. *Biochemistry*. 1982;21:6628–6633.
27. Rigobello MP, Callegaro MT, Barzon E, Benetti M, Bindoli A. Purification of mitochondrial thioredoxin reductase and its involvement in the redox regulation of membrane permeability. *Free Radical Biol Med*. 1998;24:370–376.
28. Citta A, Schuh E, Mohr F, et al. Fluorescent silver (i) and gold (i)–N-heterocyclic carbene complexes with cytotoxic properties: mechanistic insights. *Metallomics*. 2013;5:1006–1015.
29. Anderson ME. [70] Determination of glutathione and glutathione disulfide in biological samples. *Methods Enzymol*. 1985;113:548–555.
30. Du Y, Zhang H, Zhang X, Lu J, Holmgren A. Thioredoxin 1 is inactivated due to oxidation induced by peroxiredoxin under oxidative stress and reactivated by the glutaredoxin system. *J Biol Chem*. 2013;288:32241–32247.
31. Folda A, Citta A, Scalcon V, et al. Mitochondrial thioredoxin system as a modulator of cyclophilin D redox state. *Sci Rep*. 2016;6. 23071.